A DC Design of an X-band Traveling-Wave Tube

César C. Xavier
Nuclear and Energy Research Institute
São Paulo, Brazil
cesarcx@usp.br / cesarcx@gmail.com

Cláudio C. Motta
University of Sao Paulo
São Paulo, Brazil
ccmotta@usp.br

***Abstract*— In this paper a dc design procedure of a X-band traveling-wave tube is described. This procedure consists in determine the geometry of the electron gun, the periodic permanent magnetic and the electron collector. It was found that an electron gun with a 0.26 *μPerv*, 9.1 *kV*, 225 *mA* and 0.6 *mm* beam radius without electrostatic beam control was suitable for this design. The PPM, constructed with samarium-cobalt magnetics shown a good agreement with theoretical design. Finally a three stage depressed collector, to recover part of non-used electron energy and improve the overall electronic efficiency of TWT, is presented. The simulations were run with Particle-in-cell Studio.**

Keywords*— *Traveling wave tubes; periodic permanent magnets; electron gun; depressed collectors.

I. INTRODUCTION

Modern traveling-waves tubes (TWT), primarily designed for communications purposes, are considered nowadays the best solution for power microwave amplifier to be used in many commercial and military systems [1]. The TWT long-lived usage is due to its robustness, reliability and efficiency although, since 1960s, predictions indicated that sooner microwaves tube would be displaced by solid-states devices. Microwave power tubes performance for high-power transmitters is still the best choice and they will still play an important role throughout the next tube generation [2]. Also TWTs are used in many electronic systems such as space and ground based communication links.

In a typical TWT procedure designing, a scaled prototype is verified on a dedicated workbench, where the model is adjusted until design requirements are fulfilled. This procedure is time consuming and, typically, many cycles are often needed to achieve a working device which, in turns, increases its development costs. Nowadays a preferably approach is to use dedicated computer simulation tools that lead to fewer test cycles reducing the design to fewer test cycles. Many 3D codes, used to model TWTs, have been developed along the last decade such as [3]-[5].

In this work, it is presented a 0.26 *μPerv*, 9.1 *kV*, 225 *mA* and 0.6 *mm* beam radius without grids and shadow-grids TWT design using a Particle-in-cell Studio [6]. Good agreement between theoretical, simulation and experimental of a periodic permanent magnet (PPM) arrangement were observed and is also presented. The manufacturing of the electron gun, the three-stage collector and dedicated setups are under final development.

This work is organized as follows: Section II discusses, for each of the three regions (electron gun, drift tube and electron collector), the design concerns and assumptions one may take into account. The most relevant results for each region and the complete designed TWT are shown in Section III. Finally, Section IV presents the conclusions and future work.

This work was supported by FINEP (Research and Project Financing) under contract number 01.09.0049.01.

II. DESIGN CONCERNS

This section presents the main concerns to be used along the electron gun, PPM and the multi-stage collector design.

A. Electron Gun

Electron gun is used to form a suitable beam from the cathode that, at the drift region, interacts with the RF input signal. The designer challenges are: modeling an electron gun that takes into account the space charge forces, between the electrons that promotes beam's divergence (a); and providing a current density at the drift region that is far greater than the emission current that is supplied by the cathode (b). Pierce [7] developed an approach to solve these two problems considering that no magnetic field is present in the gun. Fig. 1 shows the main components of the Pierce's electron gun

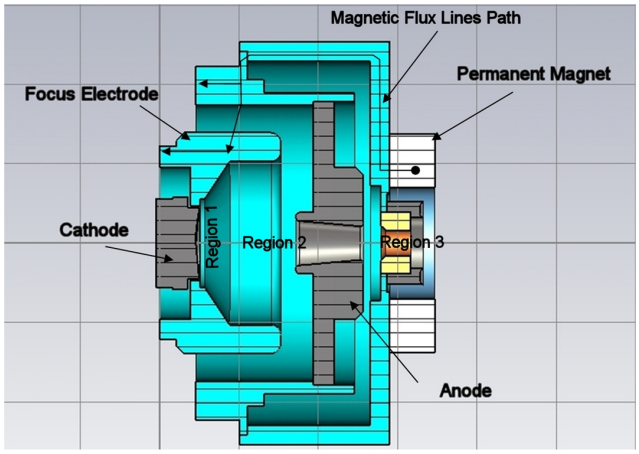

Fig. 1. Electron gun proposed by Pierce. Electron gun model overview design. High permeability materials were used to minimize magnetic field effects over the forming beam.

To get high current density a spherical cathode is used. The focus electrode is designed in such a way that the equipotential surfaces, in Region 1, must be as spherical as possible and with the same center of curvature of the cathode. Because of the anode aperture, Region 2, the electric equipotentials bow into the anode. This leads to lens effect that promotes beam divergence. In Region 3, the electron beam is no longer accelerated by the electric field of the cathode to anode regions and divergence occurs due to the space charge effect.

TWTs, typically, use a PPM arrangement to keep the beam focused along the interaction region of the drift tube. In order

978-1-4799-1397-8/13/$31.00 ©2013 IEEE

to shield the cathode, minimizing the magnetic field inside the electron gun, that would effects the beam trajectory, some materials used have high magnetic permeability. It is shown in Fig. 1 the designed solution and the preferable path used by the magnetic field.

B. PPM

Once the electron beam has been formed at the electron gun it must be confined along the drift tube. Either a PPM arrangement or a solenoid might be used to confine an electron beam. PPM is preferably used whenever weight, power and size must be minimized.

A typical PPM structure is shown at Fig. 3. This model was studied by Santra et al [8] and it was showed that the axial magnetic field B_z, for an infinite long PPM and $0 \le r < r_{f1}$, is given by:

$$B_z(r,z) = \sum_{n=1,3,\ldots}^{\infty} \frac{4B_g \sin(n\pi g/L)}{n\pi I_0(n\pi g/L)} I_0\left(\frac{2n\pi}{L} r\right) \cos\left(\frac{2n\pi}{L} z\right), \quad (1)$$

where $B_g = H_d \cdot T/g$ is the magnetic field intensity in the gap of g length, I_0 is the modified Bessel function of the first kind of zero-th order, and L is the magnet length. H_d is the magnetizing field determined from the intercept between the load line and the magnetization curve of the magnets used. The load line $K = (T/A)P_t$ is established by calculating all the magnetic circuit permeances P_t, where A is the cross-sectional area of the magnet.

It might be seem that, using (1), B_z has sinusoidal behavior at axis of symmetry (r=0).

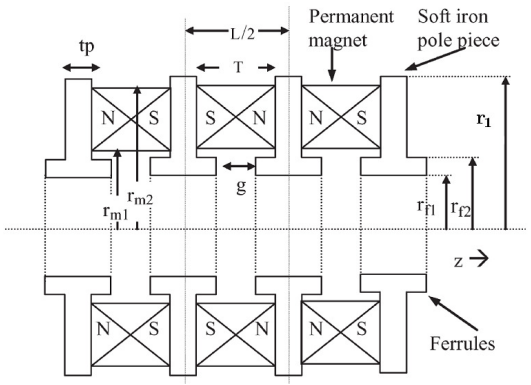

Fig. 2. PPM parameters: magnet inner radius r_{m1}; magnet outer radius r_{m2}; magnet thickness T; pole piece inner radius r_{f1}; ferrule outer radius r_{f2}; pole piece outer radius r_1; pole piece thickness t_p; gap length g; half magnet period $L/2$.

It can be shown that for the Brillouin flow to occur, at the beam waist, three conditions must be verified: the charge density must be uniform (a); no radial electron motion exist (b); and the space charge and centrifugal forces must be balanced by the magnetic forces (c). Under these assumptions, considering a uniform field, such as that produced a solenoid, Mendel [9] has shown that the Brillouin flux density B_B capable to keep a laminar flow along the drift region is given by:

$$B_B = 0.83 \times 10^{-3} \frac{I^{1/2}}{aV^{1/4}} \quad (2)$$

where I, V and a are the beam current, voltage and radius respectively. But, for a Brillouin flow occur under a PPM arrangement Mendel *et.al.* [10] had shown that the magnetic peak field B_p must be:

$$B_p = \sqrt{2} B_B \quad (3)$$

The PPM designer must also be aware of the two relevant parameters, α and β, due the magnetic field and space-charge respectively defined as:

$$\alpha = \frac{1}{2}\left(\frac{\eta B_p L}{4\pi v_z}\right)^2, \quad (4)$$

and

$$\beta = \frac{\eta I L^2}{8\pi^3 v_{z^3} a^2 \varepsilon_0}, \quad (5)$$

where v_z and η are beam velocity and electron charge-mass ratio respectively. For a Brillouin flow, in a PPM arrangement structure, $\alpha < 0.66$ must hold for a stable solution [10]. Moreover, to minimize beam ripple is desirable design α and β as low as possible. Mendel also shown that well designed PPM structures must obey:

$$\kappa = \frac{B_p{}^2 L^2}{V_0} < 2.37 \times 10^{-9}, \quad (6)$$

where V_0 is the beam dc voltage.

C. Collectors

Collector play an important role in power dissipation and recovery which are the two major considerations addressed to its design. Multistage depressed collectors (MDC) improve overall efficiency by recovering energy of the electron beam from kinetic to potential electric energy and its use is mandatory especially in satellite communications systems. Fig. 4 shows the three-stage MDC used in all simulations.

Each stage of the MDC is designed in order to decelerate the electron beam and it must be conduced in such a way to prevent electrons from being reflected. This minimizes back-streaming of secondary electrons and reflected primaries into the RF interaction region of the valve which in turn cause excessive noise, signal distortions and heating of the drift tube circuit.

CST uses Furman emission model [11] and allows designers to set the maximum number of: (a) secondary electrons per incident electron, also know as primary electron; and (b) generations, due to incident secondary electrons, to be used by the solver.

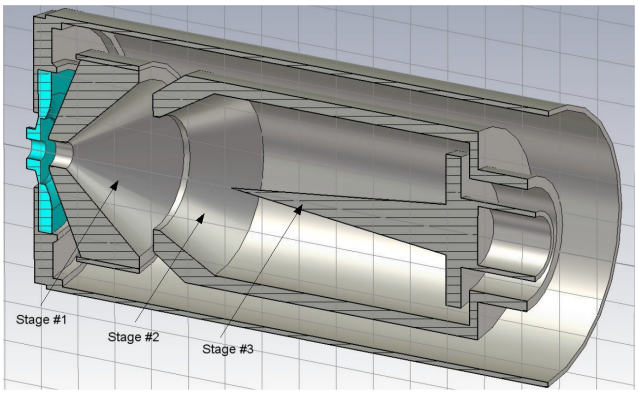

Fig. 3. Three-stage depressed collector overview.

III. Results and Discussions

All simulations were carried out on an Intel i3-2100 CPU with 3Gb RAM DDR3 under XP. On average each simulation spent 3 hours and over 60 simulations were done. Next, the relevant results are presented and discussed.

A. Electron Gun

Fig. 4 shows the beam profile generated by the electron gun under space-charge limited condition. Only two variable parameters were used to refine the results: cathode-anode separation and cathode radius. The best solution was found when the values of cathode-anode separation and cathode radius were 6.55 mm and 9.64 mm respectively. No electron hitting was observed to any part of the electron gun structure.

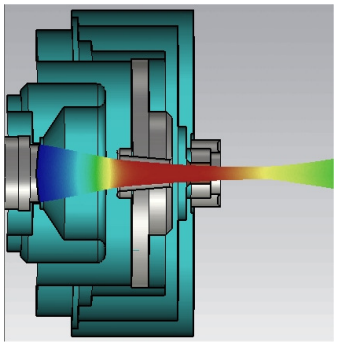

Fig. 4. Electron beam generated under space-charge limited condition with a 9.1 *kV* accelerating potential.

B. PPM

TAB. I presents the pole-piece and the magnets geometric values used according to Fig. 2. Considering the design parameters, using equation (2) and then (3), the Brillouin magnetic field and magnetic peak intensity are 0.67 and 0.95 *mT* respectively. The PPM arrangement design parameters also satisfy equation (6) where, in this case, $k = 6.65\times10^{-11}$. The parameters due to magnetic field and space charge α and β were evaluated and both satisfy stability conditions since $\alpha=\beta=0.02 < 0.66$.

A PPM with 20 (SmCo) magnets and 19 pole-pieces (Fe), of high magnetic permeability ($\mu_r \sim 5000$), was modeled with CST and the magnetic field at along the axisymmetric of the structure was benchmarked against the analytical solution (1). Fig. 6 shows the magnetic field obtained from CST and the analytical solution considering an infinite long. It might be seen good agreement between all results.

TABLE I. PPM Geometric Values Used.

Quantity	Value	Quantity	Value
r_{m1}(mm)	3.50	r_1(mm)	6.35
r_{m2}(mm)	6.9	t_p(mm)	1.23
T(mm)	2.85	g(mm)	0.95
r_{f1}(mm)	1.60	$L/2$(mm)	4.08
r_{f2}(mm)	2.60		

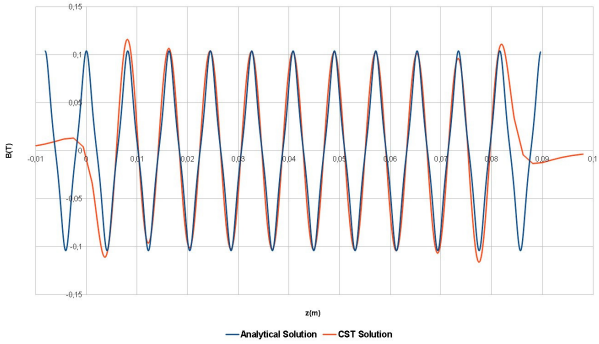

Fig. 5. Good agreement of the magnetic field observed along the axisymmetric structure of a PPM between CST and the analytical solution (1).

An experimental setup was built to measure the magnetic field profile at the center of a developed PPM arrangement with 10 permanent magnets and 11 pole-pieces, Fig. 7. The experimental setup operation is summarized as follows: an axial Hall probe (Lake Shore, Model 475), with 1 *mm* of diameter, was assembled on probe alignment system where is possible to perform a fine adjustment of the probe's horizontal and vertical position. This system, in turn, advances because it is assembled over an endless screw. The amount of translation is manually controlled, with millimeter accuracy, and read on an aligned millimeter scale.

Figure 7 shows the PPM manufactured. At left it can be seen the PPM assembled with pole pieces, magnets permanents (SmCo) and the CuBe washers. At right, it can be seen the stack of pole-piece, brazing in a vacuum furnace using copper as a filling material, together with spacers. Fe (vin-var) was used as pole-piece material due to its high magnetic permeability and the spacers were made from Monel 404 alloy. As it was not possible to find a vendor of Monel 404 alloy, at least to supply it in reasonable quantities, this material had to be developed in our facility. A procedure to prepare it, from its row materials, (copper and nickel powders), and a dedicated high temperature melting setup, dry hydrogen induction furnace were developed. After this step, the material was hot forged, annealed, roll laminated and wired-drawing in order to get a suitable diameter to be machined in a CNC lathe.

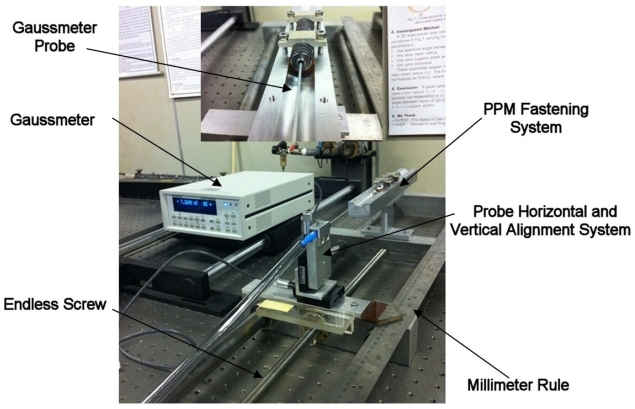

Fig. 6. Experimental setup used to evaluate the magnetic field at the center of a PPM arrangement.

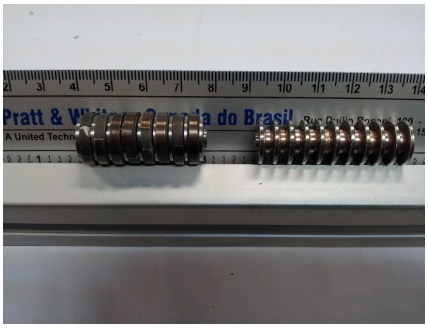

Fig. 7. PPM developed using the methodology described in Section B.

A PPM arrangement with 10 permanent magnets and 11 pole-pieces was developed with the geometric parameters presented in TAB. I. Fig. 8 shows two measurements of the magnetic field at the center of the PPM arrangement. It is possible to observe, at the center of the structure, a very good agreement of the magnetic field intensity profile between experimental, theoretical and the simulation model with CST.

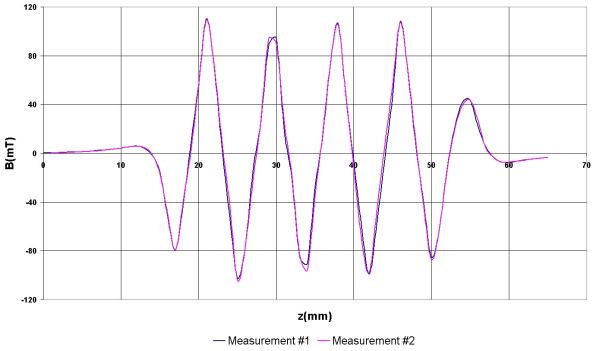

Fig. 8. Good agreement of the magnetic field observed along the axisymmetric structure of a PPM between CST and the analytical solution (1).

C. Collector

It was studied the beam behavior under voltages of the first and second stage set according to TAB. II. At all simulations the third stage voltage was fixed to 0.0 *V* and a total of 5 (five) secondary electron generations were allowed. TAB. II also shows weather or not electron back-streaming was observed at the drift tube and the total power dissipated by the collector at each configuration. The selected collector material used in all simulations was cupper.

Fig. 9 shows a typical electron back-streaming observed at the drift tube considering the first and second collector stage voltages equals to 6.37 *kV* and 910 *V* respectively.

TABLE II. THE TOTAL POWER DISSIPATED (*W*) AND WHETHER OR NOT THE ELECTRON BACK-STREAMING WAS OBSERVED AT THE DRIFT TUBE (YES/NO) CONSIDERING 12 COLLECTOR STAGE VOLTAGES (*KV*) STUDIED.

		Stage #1 voltage (*kV*)			
		7280	6370	5460	4550
Stage #2 voltage (*kV*)	910	384 Y	358 Y	336 Y	312 Y
	1820	638 Y(minor)	618 Y(minor)	625 Y(minor)	646 Y(minor)
	2730	987 N	929 Y(minor)	967 Y(minor)	980 Y(minor)

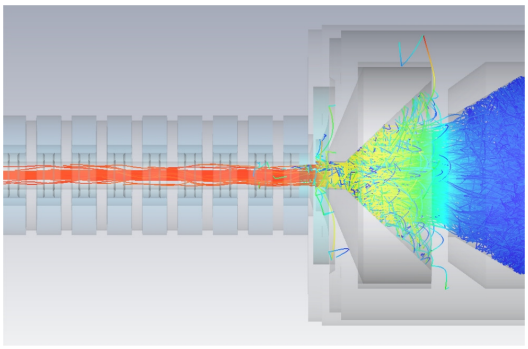

Fig. 9. Three-stage depressed collector overview.

D. TWT

The main parts of the TWT, electron gun, PPM arrangement and the electron collector, were assembled and simulated. In order to reduce the computation effort and simulation time the PPM arrangement was modeled considering 10 permanent magnets. The whole model had approximately 5.5 M meshcells. To minimize back-streaming and power dissipation, according to TAB. II, the first and second collector's stage were set to 6.37 *kV* and 1.82 *kV*, respectively.

Fig. 10(a) shows the equipotential curves along the whole TWT not considering secondary emission. It is possible to observe the accelerating and decelerating potential at the cathode-to-anode and collector region respectively. The electron beam behavior along the drift tube, from the cathode, is shown in Fig. 10(b). The electron beam profile observed at the abscissa coordinate of the center of each permanent magnet of the drift tube is presented in Fig. 10(c). Most of the evaluated electron beam profile indicates that the beam radius varies along the drift tube. That is expected since the space-

charge forces are counterbalanced by a not linear magnetic field. Another reason that justifies this behavior is attributed to the not perfect Brillouin electron beam furnished by the electron gun at the entrance of the drift tube. It is possible to observe, Fig. 7(b), that the first magnetic field plot intensity is greater than the designed and its prior behavior also affects the electron beam. Besides that, Fig. 10(c1-c2) indicates that the electron beam at the entrance of the drift tube is still converging.

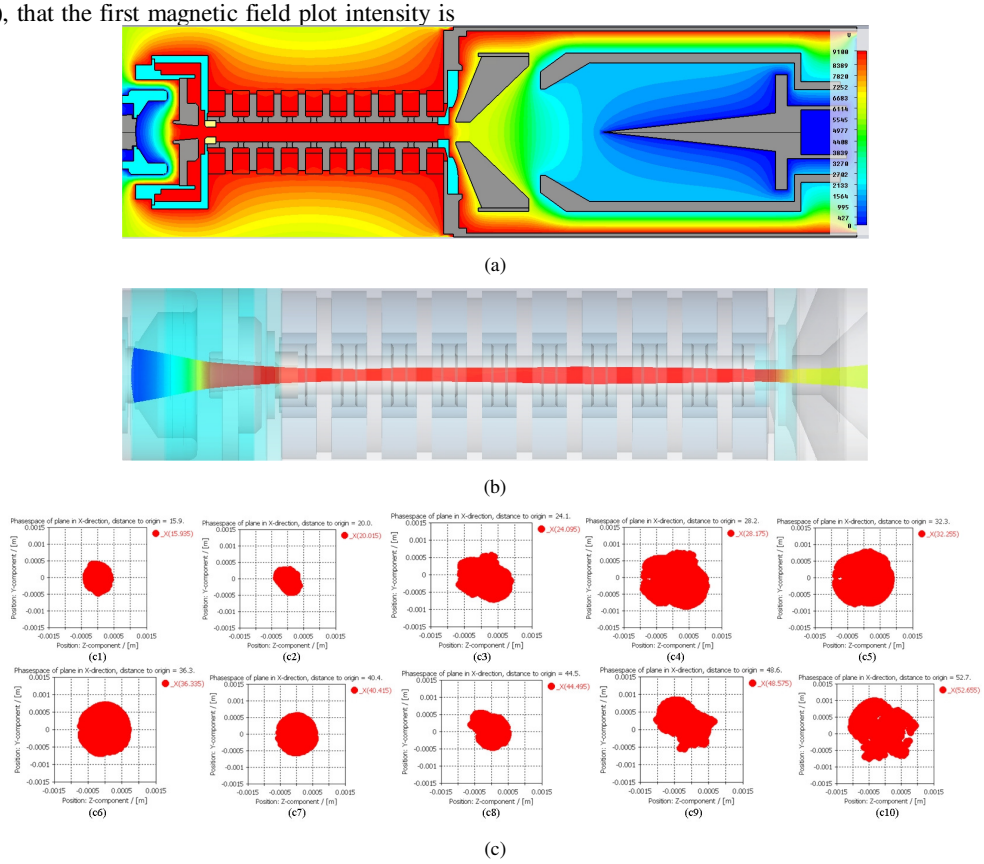

Fig. 10. TWT design overview results: equipotentials (a); electron beam behavior from the cathode along the drift tube and at the entrance of a 3 stage collector; and (c) beam profile along the drift tube.

IV. CONCLUSIONS

This work presented the most relevant DC design aspects of a TWT and its parts. It was shown that a quite well behaved electron beam may be obtained observing all design constraints. The manufacturing of the PPM parts and the dedicated setup to analyze the magnetic field at the center of the structure were presented. Good agreement between theoretical, simulation and experimental of a PPM arrangement were found. Further studies are carrying out in order to improve: (a) the electron beam formation at the entrance of the drift tube; (b) beam behavior along the drift tube; and (c) the reduction of the power dissipation at collector.

REFERENCES

[1] B. Coaker and T. Challis, "Travelling Wave Tubes: Modern Devices and Contemporary Applications," Microwave Journal, pp. 32-40, October 2008.

[2] Barker, R. Jr., *et al*, *Modern Microwave and millimeter-wave power electronics*, IEEE Press – Wiley Interscience, NJ, 2005.

[3] Petillo, J. Eppley, *et al.*, "The MICHELLE electron gun and collector modeling tool: Theory and design", *IEEE Trans. Plasma Sci.*, vol. 30, pp. 1238-1264, Jun. 2002.

[4] B. Li, *et al*. "Theory and Design of Microwave-Tube Simulator Suite", *IEEE Trans. Electron Devices*, vol. 56-5, p.919-927, Mai. 2009.

[5] S. Coco et al., "3-D Finite-Element Analysis of TWT Grid Electron Guns," IEEE Trans. Mag., vol. 43 Issue 4, pp. 1233-1236, Apr. 2007.

[6] CST – Computer Simulation Technology. Internet: www.cst.com. [May. 17,2013]

[7] J. R. Pierce, *Theory and design of Electron Guns*, 2nd ed. New York: Van Nostrand, 1954.

[8] M. Santra; L. Kumar and J. Balakrishnan, "An Improved Analysis of PPM Focusing Structures Including the Effect of Magnetic Saturation in the Iron Pole Pieces". *IEEE Trans. Elec. Dev.*, vol. 56, no. 5, pp.974-980, May 2009

[9] J.T. Mendel, "Magnetic focusing of electron beams," *Proc. IRE*, March 1955, pp.327-331.

[10] J.T. Mendel, C. T. Quate and W. H. Yocom,"Electron beam focusing with of periodic permanent magnets fields," *Proc. IRE*, Vol. 42, No. 5, May 1954, pp.800-810.

[11] M. A. Furman and M. T. F. Pivi, "Probabilistic model for the simulation of secondary electron emission," Physical Rev. Special Topics – Accelerators and Beams, vol. 5, 2002.